JOURNAL OF MATERIALS SCIENCE 15 (1980) 2046–2058

Creep and strain recovery in hot-pressed silicon nitride

R. M. ARONS*, J. K. TIEN
Henry Krumb School of Mines. Columbia University, New York, New York 10027, USA

It is observed that creep response in hot-pressed silicon is characterized by two parallel phenomena; one accounts for a persistent non-recoverable plastic deformation and the other for a transient viscoelastic recoverable deformation. The persistent creep component is time-dependent, and apparently follows parabolic time kinetics. It is further observed that creep is characterized by a power law stress exponent of about 4 and an activation energy of 848 kJ mol^{-1}. The viscoelastic recoverable component of strain is found to be independent of the total plastic strain in the material. The recovery rate at any given time is directly proportional to the preceding creep stress and therefore can be considered linear viscoelastic. The creep compliance of the viscoelastic transient is temperature-dependent with an activation energy of about 722 kJ mol^{-1}. It is further observed that the viscoelastic recovery is characterized by a spectrum of retardation times and can be modelled by a series of Kelvin analogue models. Finally, the viscoelastic recovery and the viscoelastic component of subsequent creep appear to be inversely related and apparently obey Boltzman superposition. A model is developed for the creep and recovery behaviour of hot-pressed silicon nitride consistent with all experimental observations and based in relative grain motion accommodated by the fluid grain-boundary glass liquid flow, cavitation and wedge opening.

1. Introduction

Hot-pressed silicon nitride (Si_3N_4) has generated some attention for its potential use in energy-producing systems, especially gas turbines [1–8]. In this paper we report on the time-dependent mechanical behaviour of the material. Although previous studies have failed to conclusively identify the rate-controlling mechanism for creep deformation in hot-pressed silicon nitride, it has been widely concluded that the mode of deformation is viscous grain-boundary sliding and/or boundary separation occurring via a glassy boundary phase.

This grain-boundary phase is presumed to be the combined product of oxidation and hot-pressing additives [6, 9–15], and, in the case of pressing with MgO, is believed to consist of an amorphous silicate, rich in Ca and Mg [16]. TEM studies have shown a grain-boundary phase which appears to be amorphous and which ranges in thickness from 1 to 5 nm [17]. Auger and sputtering studies have also indicated existence of a silicate grain-boundary phase of at least 2 to 3 nm thick [18]. In addition, an amorphous phase was found to concentrate at triple points [15, 16, 18–20].

It has been further recognized that, in silicon nitride, mobile dislocation-controlled deformation does not occur below 1700° C [16, 21]. Even if dislocation motion was possible, TEM studies [22] show dislocation densities far too low to account for even a small portion of observed strains in crept specimens of hot-pressed silicon nitride.

Currently, two models exist regarding the rate control of creep in hot-pressed silicon nitride; a model for creep control by non-accommodated grain-boundary sliding and relative viscous flow of the grain-boundary phase [23–25], which forecasts the existence of reasonably steady state creep, and a model where the rate control during creep is separation of boundaries governed by the flow of the viscous liquid sandwiched between grains [26],

*Present address: Argonne National Laboratory, Argonne, Illinois 60439, USA.

0022–2461/80/082046–13$03.30/0

which most certainly does not forecast steady state creep, but instead predicts a very sharp strain dependence of creep rate.

With these models and theories in mind, our study investigated creep behaviour in hot-pressed silicon nitride in the traditional manner of observing creep rate, and its functional dependences not only on temperature and on applied stress, but also with respect to its detailed time or strain dependences. In addition to the conventional creep tests, we believed that a system consisting of elastic grains and viscous glass should also display viscoelastic effects. Considering this possibility, and in light of recent understanding of the role of internal back stress in the creep of metallic systems [27], studies of transient effects in deformation were done both during creep and during strain recovery upon stress removal.

It should be noted that the conventional approach to mechanical testing of brittle materials, namely three- or four-point bending, is riddled with inaccuracies [28–30]. It samples a much smaller volume of material and assumes a symmetry of behaviour between tensile and compressive surfaces; an assumption clearly shown to be invalid in recent creep studies [23–25]. Thus all testing in this study was done in pure uniaxial tension.

2. Experimental procedure

2.1. Materials, specimen design and preparation

The material chosen for this study was NC-132*, a recent generation of hot-pressed silicon nitride with magnesia additives. The billet material was radiographed and checked for density and bending strength by the manufacturer [31]. Density was found to be 3.22 g cm^{-3}. A certification billet from the same production lot was reported to have an average three-point bend room-temperature modulus of rupture of 883.3 MN m^{-2} (128.2 × 10^3 psi). Table I shows the nominal chemical impurities in NC-132 billets as provided by the manufacturer. Major cation impurities in the starting powder for the billet material used were (by weight percent) 0.309 Fe, 0.366 Al and 0.084 Ca [31].

Specimens were diamond machined from two billets, eight specimens from one billet and four more from a second billet. Each billet set was used independently, i.e. no portion of our study relied on material from both billets. Specimens were machined with the tensile axis perpendicular to the pressing direction. Specimen design was of the buttonhead type and was adapted from a similar design used in [23]. Gauge diameter was 3.683 ± 0.003 mm and gauge length was nominally 35.6 mm. Gauge lengths and fillets were diamond-ground axially to a 600 grit finish. Specimens were photographed and enlarged and actual gauge length for each was determined from comparison with known gauge diameter. The gauge length was arbitrarily defined as that section of constant diameter between the radiused fillets.

TABLE I Nominal impurity composition of NC-132 hot-pressed silicon nitride wt % [31].

Mg	0.4 – 0.6
Al	0.18 – 0.30
Fe	0.16 – 0.35
Ca	0.006 – 0.100
Mn	~ 0.05
B	~ 0.003
W	1.5 – 2.0
O	~ 3.0

Prior to creep testing, each specimen was given a 48 h, 1010° C (1850° F) anneal in air to promote surface silica formation and surface-flaw healing to diminish the possibility of tensile failure upon loading.

Specimens for microstructural determination were cut to the necessary size (for SEM specimen holder) with a diamond saw and etched in pure HF for 16 h to dissolve grain-boundary silicates, thereby revealing grain morphology. Prior to examination they were vapour-deposited with gold to prevent static charging in the SEM. This method was considered preferable to standard ceramographic polishing and etching techniques since the latter only gives a two-dimensional view of the microstructure. The method employed is much more revealing with respect to grain size and morphology, especially when randomly oriented irregular-shaped grains exist.

The experimental apparatus is based on a dead load concept with universal couplings (two degrees of rotational freedom) at both ends of the load train. This reliably ensures that machine effects impose no bending moments common in lever-type machines. In addition, lever machines would

*The material and machined specimens were provided to us courtesy of AMMRC-Watertown through the efforts of Dr Edward M. Lenoe.

not allow unloading of the specimen without risk of unseating the specimen in the grips.

The grips used were similar in configuration to those used in the creep testing in air [23], but were of 38.1 mm diameter with round cross-section. The material used for grips was an oxide dispersion-strengthened nickel-base alloy providing the necessary creep strength and oxidation resistance through its high chromium and aluminium contents. The specimen seat was axial with the grip threads within 0.0001 in. (0.0025 mm) ensuring further minimization of bending moments. Alumina paper washers were used at the specimen seats to prevent liquid-phase hot-corrosion of either grips or specimens. In tests up to 1260° C, no evidence of alloy–ceramic intercorrosion and no bonding of ceramic paper to the specimen or grip were observed, indicating chemical stability at the specimen seats.

Specimen heating in air was achieved by use of a split furnace with molybdenum disilicide elements. This furnace afforded a ± 2° C temperature control with a 2° C gradient over the specimen gauge section. Temperature was continuously monitored with a platinum–platinum–13% rhodium thermocouple via strip chart recorder.

Strain was monitored by an extensometer comprised of two sets of high-purity alumina push rods and cross-heads which were spring loaded against the hot ends of the grips. This extensometer drove an LVDT monitored by a strip chart recorder.

The extensometry was checked in two ways. First, a secondary system was applied which sensed load train movement in the previously described fashion. Although noise in the second system was a factor of ten greater than the first due to random noise and thermal fluctuation, both positive and negative deformations were concurrently observed in both systems. A second check was performed by substituting a more mechanically stable specimen for our silicon nitride, i.e. a dispersion-strengthened nickel-base alloy, with a cross-sectional area six times greater than our standard ceramic specimen and ensuring a zero expected creep rate. The response of this system was observed under repeated loading and unloading at 1204° C with a force comparable to that utilized in silicon nitride testing. Absence of mechanical instabilities or artefacts similar to recovery on the unload cycle verified the stability of the extensometer. This test confirmed that the resolution limit of strain rate was approximately 1×10^{-9} sec^{-1}. All deformation rates that were observed to exceed this value were considered real.

In order to further assure uniaxial alignment, each specimen was instrumented with three strain gauges at 120° intervals around the specimen. The specimen was then loaded at room temperature to 17.2 MN m^{-2} (2.5×10^3 psi) and readjusted in the grips until all three strain gauges agreed within 5%. As a result, the maximum moment in these specimens for a 17.2 MN m^{-2} applied tensile stress was less than 1.5×10^{-2} MNm. The split furnace was than closed around the grips and the specimen strain gauges were observed to fall off as the adhesive volatilized, leaving no observable surface effects.

A series of hot-pressed silicon nitride specimens from the same billet were tested at stresses of 68.9, 86.1 and 103.3 MN m^{-2} (10, 12.5 and 15×10^3 psi, respectively) at 1204° C (2200° F). A similar series was tested at 1177, 1204, 1233 and 1260° C (2150, 2200, 2250, 2300° F, respectively) at 103.3 MN m^{-1} (14×10^3 psi). The following procedure was used in all cases except when otherwise stated. Immediately upon stabilization of temperature, a process taking about 1.5 h from room temperature, each specimen was loaded. Creep deformation was accumulated until 0.5% non-elastic strain was recorded, at which point the added load was removed. However, due to the weight of the bottom grip and the extensometer spring force, the lowest "zero stress" attainable was 3.13 MN m^{-2} (0.455×10^3 psi). The specimen was then allowed to recover until the change of strain with time was at a limit of resolution of 10^{-9} sec^{-1} strain rate. The specimen was subsequently reloaded to the original stress and a similar procedure of unloading and reloading was performed at 1% and at 1.5% strain unless interrupted by specimen rupture. In one test at 68.9 MN m^{-2}, at 1204° C, after the recovery at 0.5% strain, stress was increased to 120.6 MN m^{-2} for observation of creep behaviour. No subsequent unloading excursions were used. The other exception to the standard load–unload sequence was one specimen which was allowed to deform continuously to 2.25% strain before unloading.

The stress exponents and activation energies obtained through the above testing were confirmed independently by stress jump and temperature jump test techniques. These tests were conducted when the strain–time curve showed a negligible variation of strain rate within the time

frame of the stress or temperature jump experiment.

2.3. Error analysis

Systematic errors in strain–time data arise from three sources. Instrument noise associated with thermal transients and mechanical vibration place a lower limit on the resolution of extensometry. The resultant resolution of instantaneous strain was assessed at 6.8×10^{-5} and the resolution of strain rate was estimated (from the zero creep rate extensometry test) at 1×10^{-9} sec^{-1}. Apart from this noise, error in the strain and strain-rate measurement arises from error in instrumentation, i.e. error in calibration of strain recording and measurement of original specimen gauge length. This error is a constant error for each test and is estimated to be ± 2.5% measured strain or strain rate. A third source of error is in experimental variables of stress, temperature and time. The error in measured strain rate has been estimated for creep to be ± 11% of the measured value, and for recovery to be ± 8% of the measured value. The total error in any measured strain rate was assumed to be the sum of these three errors.

In the course of data analysis, functional dependencies of external variables upon strain or strain rate were frequently evaluated from regression-curve fitting by conventional least-squares techniques. Standard error values, as computed from statistical correlation of data, were reported as confidence limits in functional parameters such as activation energy or stress power law exponents.

3. Results and discussion

3.1. Materials characterization

Fig. 1 shows an SEM of NC-132. The majority of grains appear elongated and prismatic, ranging from 3.0 to 11.5 μm long and from 0.2 to 2.5 μm wide. This estimate is subject to some error since with such a fibrous and random microstructure, it is impossible to observe the full length of most grains since they extend into the bulk.

3.2. Creep results and analysis

3.2.1. General behaviour.

Briefly, it has been found that (1) no steady state creep is observed, but instead the strain apparently follows power law time kinetics, (2) viscoelastic recovery and an associated viscoelastic transient upon reloading are observed, and (3) the non-recoverable component of creep, which will be defined as persistent creep deformation, appears to accumulate simultaneously and non-sequentially to the viscoelastic component.

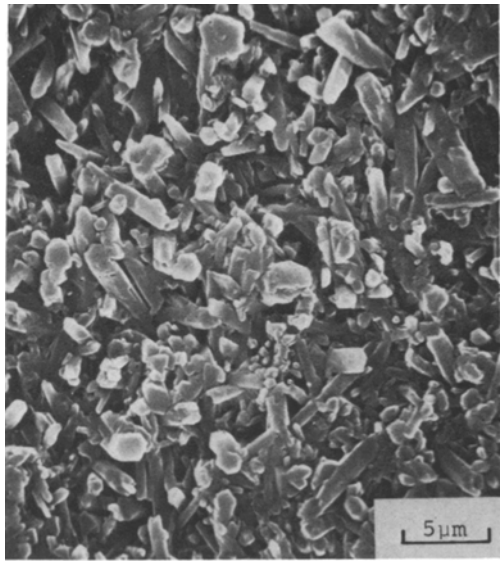

Figure 1 SEM of etched hot-pressed silicon nitride (NC-132) showing prismatic elongated grain structure. Apparent voids in the structure are the result of dissolution of silicates during etching in HF and pull-out of grains during preparation.

3.2.2. Time-dependence of creep

The general creep curve shape is presented in Fig. 2*. Specimen 2 is a test taken to 2.25% strain without any strain-recovery interruptions. Specimen 6 gives a similar plot, but was constructed as a composite, piecewise from the components of persistent creep deformation (i.e. with visco-

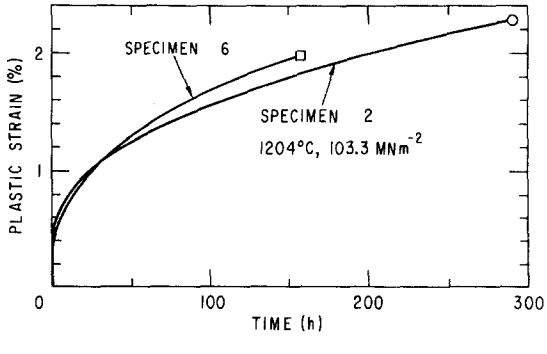

Figure 2 Representative creep curves illustrating general curve shape. Curves taken from specimens crept at 1204° C, 103.3 MN m^{-2} to failure. Note lack of steady state or tertiary behaviour.

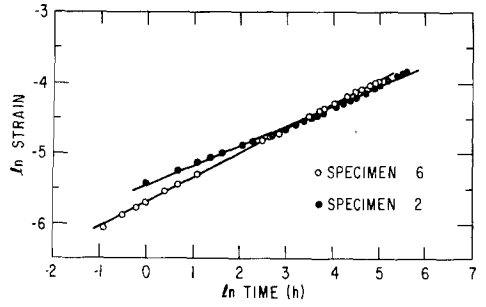

Figure 3 Creep curves shown in Fig. 2 replotted on a log–log scale. Quality of straight-line fit illustrates power law dependence of strain upon time.

elastic transients removed) versus time under load. The resultant curve which is continuous and of similar shape as Specimen 2 illustrates that persistent creep and viscoelastic transients are parallel reactions and can be treated independently. (Further justification for this assertion will be provided in a later discussion.) Contrary to the reports of other comprehensive studies of creep in hot-pressed silicon nitride, [23–25, 32], a steady-state regime was never reached in any of our tests with times as long as 405 h, or strains as high as 2.25%. Similar behaviour has been reported in only one other study of hot-pressed silicon nitride when tested in bending [33], but only a few tests were performed and never beyond 50 h.

The nature of the time-dependence of creep becomes evident in Fig. 3 where the log of creep deformations of Fig. 2 are plotted against the log of time. The high-quality of a straight line to the logarithmically plotted data illustrates a power law time dependence of creep following the expression

$$\epsilon = at^b \tag{1}$$

where b is the least-square fit slope of the log–log plot and a is the value of strain, ϵ, at $\log t^b = 0$. We find that both a and b are constants for any given isothermal, constant stress test. Values of a and b are tabulated in Table II. Comparing data from specimens 2 and 6, at the same stress and temperature, scatter in the value of b is 0.06 in about 0.3 and scatter in a is 0.0008 in about 0.004. Upon examination of tests done at different temperatures or stresses, excluding no. 5, any dependence of b or a upon stress or temperature is weak and irresolvable within the defined limits of scatter. The results from test 5 may not be trustworthy, as seen from the results in Table II, since an extremely short life (~ 10 h) was observed and, as a consequence, the creep curve may or may not have exhibited a tertiary stage of creep.

It follows from Equation 1 that the creep rate is also a power function with time [34] since upon differentiation of Equation 1 we get

$$\dot{\epsilon} = abt^{b-1} = c\epsilon^d. \tag{2}$$

It should further be noted that, as b approaches unity or as t gets longer, $\mathrm{d}\dot{\epsilon}/\mathrm{d}t$ as given by

$$\ddot{\epsilon} = ab\,(b-1)t^{b-2} \tag{3}$$

becomes very small and a creep curve so derived would appear to approach a straight line easily mistakable for steady-state creep upon casual inspection. However, when the creep curve is decreasing very gradually with time, errors will arise by assuming a "steady creep rate" from the apparently constant rates attained early in a creep test.

Another commonly used empirical expression, which has been reportedly successfully applied to glass-bonded silica refractories [35], is

$$\epsilon = (\sigma/k_2)(1 - \epsilon^{-k_1 k_2 t}) + k_3\,(\sigma - \sigma_0)t \tag{4}$$

where $k_{1,2,3}$ are constants at constant temperature, σ is the applied stress, and $\sigma_0 \geq 0$ is an apparent yield stress. This expression is founded on the summation of a primary creep as defined by

TABLE II Curve fit parameters from $\epsilon(t) = at^b$

Specimen	Temperature (° C)	Stress (MN m^{-2})	b	a
7	1204	68.6	0.265 ± 0.002	0.002 615 ± 0.000 03
9	1204	86.1	0.273 ± 0.003	0.003 455 ± 0.000 10
2	1204	103.3	0.292 ± 0.004	0.004 090 ± 0.000 14
6	1204	103.3	0.354 ± 0.002	0.003 247 ± 0.000 08
8	1177	103.3	0.303 ± 0.003	0.002 951 ± 0.000 11
3	1233	103.3	0.352 ± 0.005	0.003 660 ± 0.000 16
5	1260	103.3	0.503 ± 0.023	0.007 880 ± 0.000 45

$(d\epsilon_p/dt) = k_1(\sigma - k_2\epsilon)$, in which a back stress of $k_2\epsilon$ increases with ϵ, and a steady-state creep where $\epsilon_s = k_3(\sigma - \sigma_0)t$. This equation does not apply to our observed creep curves, however. Notable weaknesses of this equation are the failure to fit high initial creep rates and the complete inability to rationalize continued $\epsilon(t)$ curvature ($\ddot{\epsilon}$) at long times.

Furthermore, no expression similarly derived as Equation 4 could fit the observed creep curve. Any analysis which views the creep rate as a sum of a primary creep, $\dot{\epsilon}_p$, and a steady state creep, $\dot{\epsilon}_s$, would imply that the value of b in Equation 1 could not be constant, but would approach $b = 1$ gradually as a steady state is obtained. We have clearly shown this is not the case; b is constant witth time and not equal to one as shown in Fig. 3. It must, therefore, be concluded that no evidence for the existence of any steady-state contribution to creep was found.

3.2.3. Temperature-dependence of creep

The general approach to obtaining temperature-dependence of creep kinetics is through the use of the phenomenological expression,

$$\dot{\epsilon} = Af(s)\sigma^n \exp(-Q/RT) \qquad (5)$$

where A = constant, $f(s)$ = some function of creep structure, σ = applied stress, n = a power law exponent of applied stress, Q = activation energy for creep and is usually compared with those for various diffusional or transport processes for mechanistic discussion purposes, and RT is the product of the gas constant and absoulte temperature. Accordingly, Q is obtained by holding all other variables constant while varying temperature in a series of creep tests.

In the case where creep rate also varies the time, i.e. where no steady state exists, as in our case, it is not clear what choice of creep rates should be used. All that is certain is that $f(s)$ or the creep structure should be held constant [27, 36], as temperature is varied. This poses a problem since any observed variation of creep rate during an isothermal–constant stress test is indicative of a changing internal structure. In other words, $f(s)$ would be constant only if b in Equations 1 and 2 is equal to 1, and steady-state creep is observed, contrary to our case.

Various investigators have asserted that constant structure exists at constant strain in fireclay refractories [37], high-purity alumina [38], and even reaction-sintered silicon nitride [39]. Another investigator has, on the other hand, assumed that structure is time-dependent in analysing of UO_2 [40, 41].

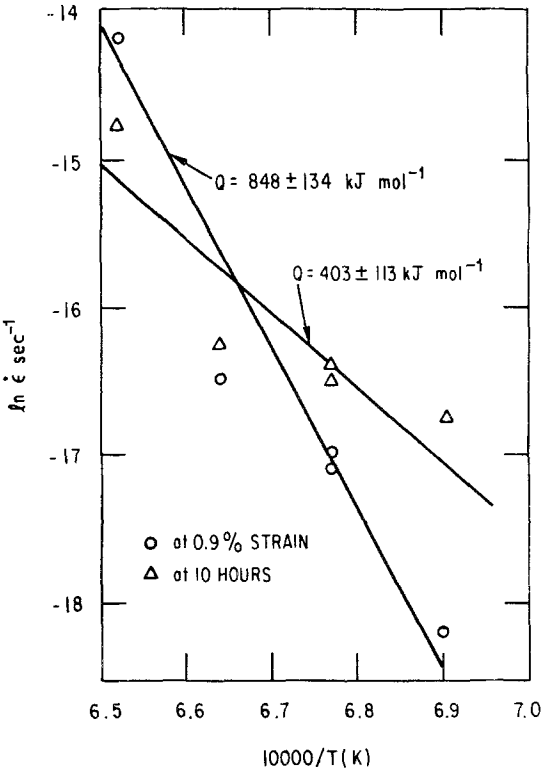

Figure 4 Temperature-dependence of creep rate taken at both constant strain (0.9%) and at constant time (10 h) for specimens crept at 103.3 MN m^{-2}.

Both methods were applied to the creep data generated in this study. Fig. 4 shows a log plot of strain rates versus reciprocal absolute temperatures at constant stress of 103.3 MN m^{-2} and creep strain of 0.9%. The activation energy, Q, obtained in this manner was 848 ± 134 kJ mol^{-1} (202 ± 32 kcal mol^{-1}). Similar analysis at a different strain of 0.75% yields essentially the same value for Q, 853 ± 185 kJ mol^{-1}. This is in fair agreement with the value of 706 kJ mol^{-1} found for NC-132 [25], the same material as in this study but crept in vacuum. It is, however, higher than values observed in HS-130 (~ 546 kJ mol^{-1}), a similar material with higher impurity content [23, 24]. However, it must be noted that both groups of investigators approximated their creep curves as straight lines in obtaining the Qs.

Fig. 4 also shows a plot at constant time (10 h). This plot, which displays much more scatter than the constant strain plot, yields an activation

energy of 403 ± 113 kJ mol^{-1}. Performing a similar analysis at different choices of constant time yields values ranging from 294 to 403 kJ mol^{-1} *.

As a check on either of the above approaches, Q can be evaluated experimentally from data at two temperatures via the relation,

$$Q = \frac{R \ln (\dot{\epsilon}_1/\dot{\epsilon}_2)}{(1/T_2) - (1/T_1)}. \quad (6)$$

Using this relation, we can determine Q from temperature-jump experiments on a single specimen. Here a specimen is crept to a finite strain, and at constant stress the temperature is abruptly changed and variation in creep rate is observed. This sequence is believed to provide essentially constant structure and creep rates are compared at essentially the same time and strain, thus circumventing the previously described potential conflicts. As mentioned, such an experiment was carried out on a specimen with significant creep strain so that variation in creep rate with time would be negligible over the time frame considered. For a temperature change of 1204 to 1260° C at a stress of 86.1 MN m^{-2}, an activation energy of $Q = 819 \pm 84$ kJ mol^{-1} (195 ± 20 kcal mol^{-1}) was obtained. This is in close agreement with that obtained in the Arrhenius plots with constant strain.

3.2.4. Applied uniaxial stress-dependence of creep

Using arguments similar to those presented in the previous section, the stress exponent, n, in Equation 5 should be obtained at a constant structure. Again, for lack of assurance on how to define constant structure, both "constant strain" and "constant time" analyses were done on creep data from individual specimens. Fig. 5 shows a log–log plot of strain rate versus stress at a constant temperature of 1204° C and creep strain of 0.5%. Owing to the limited number of specimens, only a four-point data set was obtained. The stress exponent from this data was 4.1 ± 0.5. Use of a higher strain (0.9%) required the use of data from one stress-jump experiment where the change in stress occurred at 0.5% strain as described in Section 2. This yielded a consistent value of 5.5 ± 1.1 for n. High stress exponents were found by Kossowsky *et al.* in previous study as shown in Fig. 8 of [24] in the high-stress regime. In that investigation, however, creep curves were approximated as straight lines in obtaining creep rates for n.

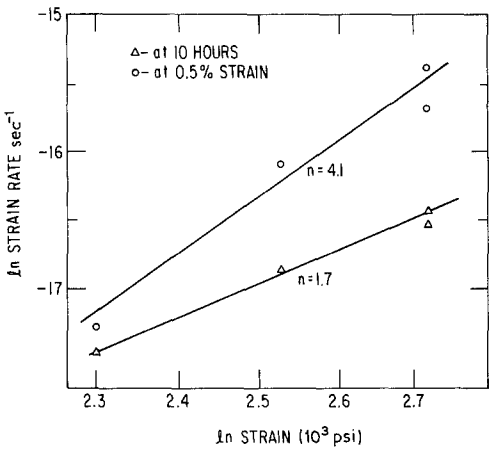

Figure 5 Stress dependence of creep rate taken at both constant strain (0.5%) and constant time (10 h) for specimens crept at 1204° C.

Fig. 5 also shows a plot with time held constant (at 10 h) for extraction of creep rates. The value of n from this analysis is 1.7 ± 0.1. Contrary to the case of temperature-dependence, use of different time choices for constant time did not alter this values significantly, e.g. use of 1 h gives $n = 1.3$.

Alternately, in a manner analogous to the temperature-change experiments, n was also evaluated from data at two stresses via the relation $n = \ln (\dot{\epsilon}_1/\dot{\epsilon}_2)/\ln (\sigma_1/\sigma_2)$. For a stress-change effect on a creep test at a temperature of 1204° C and stresses of 103.3 and 120.1 MN m^{-2}, a stress exponent of 3.5 ± 0.8 was found. This value is in good agreement with the values 4.1 ± 0.5 and 5.5 ± 1.1 as found in the constant strain rate case, but is higher than the values found with time held constant.

3.3. Viscoelastic recovery and transients

3.3.1. General approach and behaviour

As presupposed, recovery occurred and was characterized by extremely high initial rates which rapidly decreased as seen in Fig. 6, a representative recovery curve. After about 3 h, the rate slowed and the recovery rate gradually approached the limit of resolution (10^{-9} sec^{-1}). Generally, the total recovered strain approached 0.1% absolute strain, or roughly 5 to 10% of the previous creep strain

*It may be argued that data scatter about the straight lines in Fig. 4 would cast some doubt on the validity of the data point at the highest strain rates. If that point were discarded from both plots, the reported activation energies would certainly be lower, but would still be roughly a factor of two greater than that evaluated at constant time.

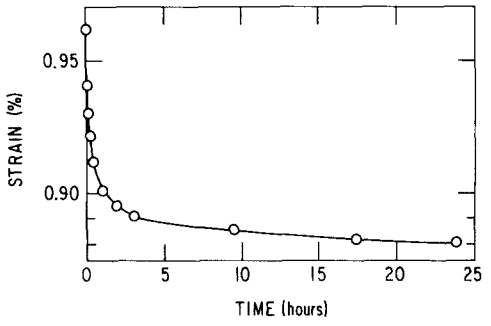

Figure 6 Strain versus time curve for recovery at 1204° C; prior stress 103.3 MN m^{-2}.

and recovery lasted up to 30 h, although continued recovery at about the limit of resolution was observed in some cases over 100 h.

When the specimen is reloaded, the curve displays an inverse of the recovery in parallel and along with the continued accumulation of non-recoverable plastic deformation. Since it is not possible to separate this viscoelastic component of stress from the much more intense persistent creep phenomenon, no direct evidence is available that this is precisely an inverse of the preceding recovery curve. However, our success with creation of composite creep curves as previously described, is consistent with the notion that viscoelastic behaviour on reloading is directly opposite that of recovery and one full cycle yields only that strain due to persistent creep.

3.3.2. Results of recovery

The results of the strain–recovery experiments are presented in Table III. The results presented are not for total load removal since the load strain stress of 3.13 MN m^{-2} remained. Under these conditions certain trends are observed. Recovery from varying strains at 1204° C and 103.3 MN m^{-2} in specimens 2 and 6 show recovery to be essentially independent of accumulated strain. From experiments performed at 1204° C at varying stresses, it is apparent that the recovery rate is dependent upon stress before recovery and increases (let us define a greater negative strain rate as an increasing recovery rate) with increasing stress. At constant stress, but varying temperature, the recovery rate appears to proceed through a maximum at the intermediate temperature of about 1204° C. (In fact, the recovery rate at 1260° C, 103.3 MN m^{-2} is actually a positive strain rate.) Examination of the strain–time curve for this particular recovery experiment showed a recovery of roughly 0.05% strain in 0.5 h, after which the curve turned upward and the positive strain rate was observed.

Since the apparent recovery rates reported in Table III are those rates resultant from recovery and creep under a small load, the effect of that small load needs to be factored out. One approach to correct the results of recovery tests with a small residual load would be to develop complete creep curves under the grip weight and extensometry force at every temperature employed and through the appropriate maximum time period or strain necessary. The creep rate under the low stress could then be subtracted from the recovery strain rate, separating the superposition curve observed, and yielding the appropriate corrected recovery. This approach is unreasonable due to the enormous investment of time; for example, a

TABLE III Recovery data

Specimen	Temperature (° C)	Stress (MN m^{-1})	Accumulated strain (% ± 0.05)	Recovery rate* at $t = 4$ h (sec^{-1})	Recovered strain (%)	Duration (h)	Corrected recovery rate (sec^{-1})
7	1204	68.9	0.50	-1.7×10^{-9}	0.020	4	-2.4×10^{-8}
9	1204	86.1	0.50	-5.0×10^{-9}	0.062	19	-2.7×10^{-8}
2	1204	103.3	0.25	-1.5×10^{-8}	0.178	118 +	-3.7×10^{-8}
6	1204	103.3	0.50	-1.2×10^{-8}	0.090	18	-3.4×10^{-8}
6	1204	103.3	1.00	-1.0×10^{-8}	0.080	24	-3.2×10^{-8}
6	1204	103.3	1.50	-1.5×10^{-8}	0.085	10	-3.7×10^{-8}
8	1177	103.3	0.50	-4.1×10^{-9}	0.058	22	-1.0×10^{-8}
3	1233	103.3	0.50	-5.9×10^{-9}	0.064	8	-8.5×10^{-8}
3	1233	103.3	1.00	-6.3×10^{-9}	0.132	32	-8.5×10^{-8}
5	1260	103.3	0.50	$+1.0 \times 10^{-8}$	0.050†	1†	-2.6×10^{-7}

*Recovery rate taken at 4 h after load removal.
†Before turnabout in curve (see text).

creep test at 3.13 MN m^{-2} and 1177° C could take over 10^4 years to reach 1% strain.

Another approach to this problem, and the one we used is to produce one partial creep curve at the highest temperature of 1260° C under the low stress in a virgin sample, assume that to be the true contribution to the apparent recovery rate at 1260° C, and then extrapolate the expected creep contributions at other temperatures through the measured temperature-dependence of creep rate, i.e. through use of the determined Q value of 848 kJ mol^{-1}. This allows for correction of recovery data presented in Table III.

The creep test run at 1260° C under just the fixture stress showed a reasonably constant creep rate of 2.75×10^{-7} sec^{-1} in a virgin specimen. This value was defined as the low stress contribution to the superposition of creep and recovery at 1260° C. Using the measured value for activation energy for creep of 848 kJ mol^{-1} (202 kcal mol^{-1}), the contribution of creep to the observed recovery strain rates at 1177, 1204, 1233 and 1260° C are calculated as 6.1×10^{-9}, 2.2×10^{-8}, 7.9×10^{-8} and 2.7×10^{-7} sec^{-1} respectively.

The corrected recovery data are also presented in Table III. Recovery rates are arbitrarily reported as the strain rate at 4 h after load removal.

From Table III, it is apparent within data scatter, that recovery rate is independent of prior strain in the material at a constant prestress and temperature. It is further evident that although creep rates vary with strain in the material, recovery rates are also independent of prior creep rate. It is concluded then that prior strain history does not affect transient viscoelasticity, providing of course that previous transient behaviour is complete before changing stress conditions. In addition, repeated load and unload cycles result in recovery curves of the same shape.

Fig. 7 shows a plot of normalized corrected recovery rate versus normalized prior creep stress at constant strain and temperature. The linear dependence with a slope of 1.1 ± 0.2 demonstrates that the recovery phenomenon is linear viscoelastic.

The most general and simplest linear viscoelastic analogue model which predicts a creep transient and subsequent recovery is the Kelvin (or Voight) model consisting of a spring and dashpot connected in parallel. Under a step loading function, $\sigma = \sigma_0 H(t)$, where σ_0 is the applied stress and $H(t)$ is a unit step function, the resultant strain is

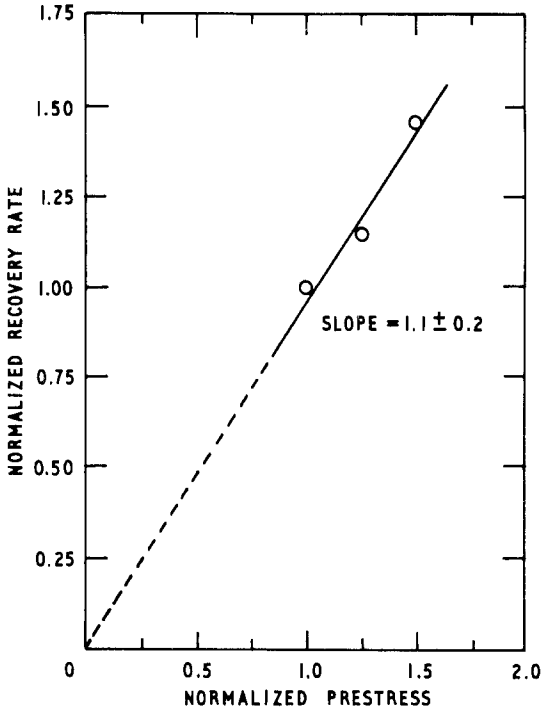

Figure 7 Dependence of corrected recovery rate upon prior stress. Curve slope of ~ 1 is indicative of linear viscoelasticity.

$$\epsilon(t) = [1 - \exp(-t/\theta)]\,\sigma_0/k, \qquad (7)$$

where θ, the retardation time, equals n/k, the dashpot viscosity divided by the spring constant. The quantity $[1 - \exp(-t/\theta)]/k$ is usually denoted by $C(t)$, and is called the creep compliance function. Equation 7 than becomes

$$\epsilon(t) = C(t)\sigma_0. \qquad (8)$$

Upon removal of the stress at time $t = t'$, the

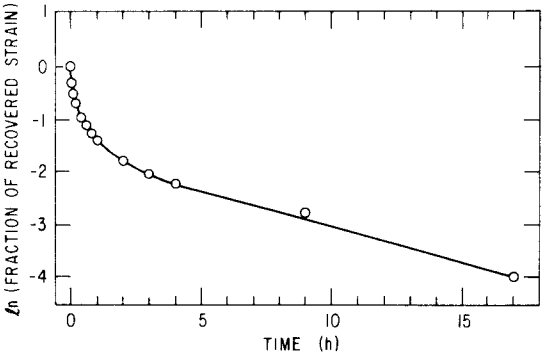

Figure 8 Plot of natural log of the fraction of recovered strain versus time. Lack of straight line fit indicates that recovery is characterized by a spectrum of retardation times.

superposition principal demands that for $t > t'$

$$\epsilon(t) = \epsilon(t') - C(t - t')\sigma_0. \quad (9)$$

This model predicts that a plot of $\ln \{[\epsilon(\infty) - \epsilon(t)]/\epsilon(\infty)\}$ versus t will yield a straight line plot of slope $= \pm \theta$. A plot of this type is shown in Fig. 8. Lack of a straight-line plot is evidence that the recovery process is not characterized by single retardation time. Instead, it is necessary to represent the material as a finite series of Kelvin models (e.g. [42]) with a spectrum of retardation times. Hence, the creep compliance becomes,

$$C(t) = \sum_i (1/k_i)[1 - \exp(-t/\theta_i)] \quad (10)$$

and Equations 8 and 9 are still valid.

The activation energy for the viscoelastic process is obtained through the temperature-dependence of the recovery rate. The activation energy for the viscoelastic mechanism can be obtained by allowing

$$Q_v = -\{[\partial] n\dot{C}(t,T)]/[\partial(1/RT)]_{t=\text{const.}} = -[\partial] n\dot{\epsilon}(t,T)]/[\partial(1/RT)]_{t=\text{const.}}\} \quad (11)$$

The natural logarithm of recovery strain rate versus reciprocal absolute temperature is plotted in Fig. 9. The resultant activation energy is $Q_v = 722 \pm 25$ kJ mol^{-1} (172 ± 6 kcal mol^{-1}) at 4 h.

The data used in Fig. 9 were taken at 4 h after load removal. Data taken similarly at 2 h after load removal yield a similar result of $Q_v = 709 \pm 41$ kJ mol^{-1}.

The calculations for activation energy were repeated for data taken at equivalent recovered strains rather than at equivalent times after load removal. Data taken at total strain recoveries of 0.05% and 0.033% yielded calculated activation energies of 745 ± 188 and 792 ± 217 kJ mol^{-1}, respectively. Hence, data taken at either choice of constant strain or at a different choice of constant time all yielded values of activation energy which agree with our reported 4 h value within 10%.

The calculated value of viscoelastic activation energy, Q_v, of 722 kJ mol^{-1} is lower than the activation energy found for the persistent creep process, Q_c, of 848 kJ mol^{-1}. However, the conclusion that $Q_c > Q_v$ would be based on circular reasoning since Q_c was used in data correction for calculation Q_v. This is reflected by the original recovery data, Table III. If both recovery and creep were characterized by the same activation energy, dominance of one mechanism over the other would not be temperature-dependent. The fact that the creep effect is only dominant at higher temperatures indicates that it has a stronger temperature-dependence and, hence, a higher Q.

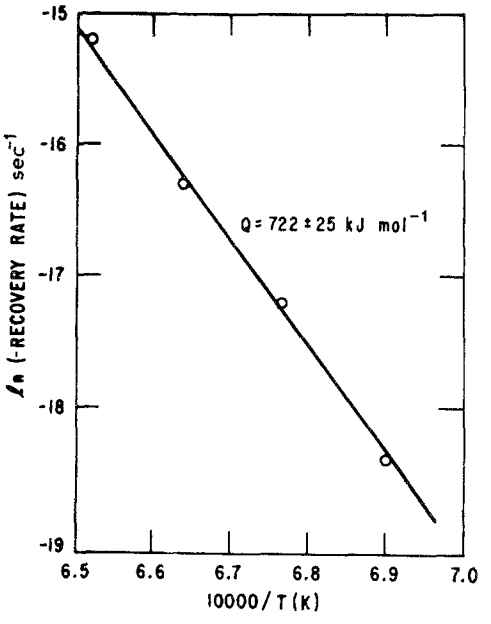

Figure 9 Temperature dependence of corrected recovery rate.

5. Discussion of mechanism

Based on the observed applied stress, temperature, strain and time dependence of creep strain recovery, and on suggestions extracted from previous models [23–26], we visualize that upon loading and after the initial elastic deformation, the grains will begin to slide relative to one another under resolved shear stresses. The relative motion of grains will result in large pressure gradients in the grain-boundary liquid phase since the deformation process is inhomogeneous, i.e. grains are not significantly plastically deforming while intergranular regions are. These pressure gradients should result in either (1) glassy fluid flow from a region of high pressure to one of lower pressure, or (2) opening of voids (or wedges) in the lower pressure regions due, say, to the absence of sufficient fluid or hindered flow. The grain-boundary sliding would then be a sequential machanism with the accommodating fluid mechanism, and the overall apparent creep kinetics can then be visual-

ized to be determined by characteristics such as fluid viscosity and distribution.*

As creep deformation progresses, it is proposed that grains will rearrange and rotate, resulting perhaps in an improved grain packing along shear planes. Accordingly, contact areas between the grains will increase, thus increasing resistance to sliding while reducing the cross-section of existing paths for fluid movement. We maintain that this condition should result in a strain-hardening effect, i.e. an ever-changing (decreasing) creep strain rate, consistent with our experimental observations. It is interesting to note that a similar hardening effect has been observed in a model system of sand bonded with viscous fluid [35], lending credence to this view of hardening in our system of fluid-bonded grains.

The observed stress-dependence with a stress exponent of about 4 may also be resolved within the framework of our model. When such a system does respond by growth of voids in the regions of high negative pressure, these regions will have less resistance to further deformation and will support a smaller fraction of the applied load. If the number of void-containing regions is a function of stress, then at higher applied stresses the volume fraction of voids should be greater. Hence, as stress is increased, not only do voidless regions bear the larger applied stress, but also a larger fraction of the applied stress.

A model for stress dependence of creep in a system with stress-induced void growth has previously developed [43] for partially amorphous glass ceramics and may, in principle, be applied to silicon nitride. According to that model, any given volume of the aggregate will contain x_0 number of glassy areas of which $x(\sigma)$ contain voids under an applied stress, σ. If each void containing glassy regions affects y nearest neighbour regions such that they have negligible resistance to deformation compared to voidless regions, then the voidless material must support a greater stress by a factor of $x_0/x_0 - yx(\sigma)$. If we assume that grain-boundary sliding and grain-boundary fluid motion vary with stress, then the aggregate creep rate is given as:

$$\dot{\epsilon} = \text{constant} \cdot \sigma \frac{x_0}{x_0 - yx(\sigma)}. \qquad (12)$$

The stress exponent defined by $n = \ln \dot{\epsilon}/\mathrm{d} \ln \sigma$ is then given by:

$$n = 1 + \frac{y}{x_0 - yx(\sigma)} \frac{\partial x(\sigma)}{\partial \sigma}. \qquad (13)$$

Although the parameters x_0, y, and $x(\sigma)$ are unknown in this material, it has been shown that reasonable values for these parameters in glass ceramics and firebrick may yield theoretical n values between 1 and 6, and n may be a reasonably strong function of stress [43].

In our proposed model, the temperature-dependence of the kinetics of glass flow should be controlled by the activation energy of the viscosity of the glass phase. The observed creep rates also may depend upon the number of voids within the glass phase which again should be temperature-dependent, reflecting stress-induced and thermally activated deformation and/or growth of these voids. As a result, the apparent activation energy for creep should, in principle, be a function of the energies for both these thermally dependent processes. Accordingly, it is reasonable that the observed value of creep activation energy of 848 kJ mol^{-1} is greater than the 625 to 764 kJ mol^{-1} range of activation energies measured for the viscosity of the glass phase by internal friction techniques [44]. At this time we have no way of estimating the contribution due to the voids.

Simultaneous to the plastic deformation by glass flow and grain motion, elastic stresses slowly build up in the non-deforming grains. An exaggerated schematic illustration of this behaviour is presented in Fig. 10. At time $t = 0$, the entire stress is supported by viscous liquid and elastic grains. As time progresses, the liquid flows from regions of high pressure, denoted by A, to regions of lower pressure as described previously. As this flow occurs, the grains must support a larger stress and respond by further elastic deformation. Also, as this flow occurs the pressure at A will decrease.

Upon subsequent unloading (and after immediate elastic response of the composite system), the relief of that elastic stress, which was stored by the gradual elastic deformation of grains just described, is resisted by capillary adhesion again

*Experimental evidence suggests that the grain boundary glass phase may not be homogeneously distributed on all grain boundaries [17, 20], but instead may be concentrated along grain-boundary triple points (or, more properly, triple line junctions). The deformation model suggested will still be valid, despite the glass-phase distribution, if the glass phase is continuous and glass is allowed to flow from high-pressure reservoirs to low-pressure reservoirs during relative motion of grains.

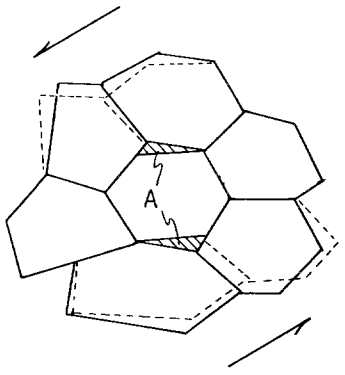

Figure 10 Exaggerated schematic illustration of proposed viscoelastic deformation model. Regions A represent liquid glass phase.

at point A. As liquid returns to location A, strain recovery should be observed as the intragranular elastic stresses relax.

As mentioned, this viscoelastic behaviour can be modelled by a simple Kelvin model (or series of Kelvin models) where the dashpot viscosity is related to the viscosity of the liquid phase and will display the same temperature-dependence. Consistent with this argument, our observed activation energy of recovery of 735 kJ mol^{-1} is in excellent agreement with those values reported for boundary-phase viscosity of 625 ± 764 kJ mol^{-1} [44]. The deformation rate at any given time should also be directly proportional to the applied stress, assuming Newtonian response of the liquid. This again is consistent with the physical observation as shown in Fig. 7.

If the hot-pressed silicon nitride is again step loaded after the loading–unloading cycle has been completed, once again the elastic strains will accummulate and we visualize that the grains will continue to slide and rearrange as before, and the persistent creep deformation will simply continue from where it was interrupted by the unloading sequence.

One might also argue that, despite the grain rearrangement which takes place during the persistent creep deformation, there will always be wedges or pockets of fluid as depicted at region A in Fig. 10. Following this argument, one might suspect that the viscoelastic phenomena should be relatively independent of accumulated plastic strain. Although this argument is consistent with our experimental observation, it is speculative and requires further refinement.

Accordingly, it is proposed that creep deformation in hot-pressed silicon nitride is due to relative grain motion accommodated by grain-boundary phase flow and cavitation. An observed viscoelastic transient is explained by an elastic strain controlled by percolating flow of the grain-boundary phase. Retardation times of this transient are dependent upon the viscosity of this phase and display the same temperature-dependence as this viscosity. The persistent creep deformation is explained by grain-boundary sliding which is rate-controlled and accommodated by grain-boundary phase percolation and cavitation void and wedge opening. All evidence points to the conclusion that the hardening behaviour is strain-controlled, rather than time-controlled. Variation of grain packing and arrangement or local stress distribution probably plays a role in the observed strain hardening.

Acknowledgement

We wish to thank EPRI, Palo Alto, California for sponsoring this research. We are also grateful to Dr E. M. Lenoe of AMMRC-Watertown for his help.

References

1. E. C. VAN REUTH, The advanced Research Projects Agency's Gas Turbine Program, in "Ceramics for high performance applications", edited by J. J. Burke, A. E. Gorum and R. N. Katz (Brook Hill, Chestnut Hill, Mass., 1974) pp. 1–5.
2. A. F. MCLEAN, Ceramics in Small Vehicular Gas Turbines, *ibid.* pp. 9–36.
3. R. J. BRATTON and A. N. HOLDEN, Ceramics in Gas Turbines for Electric Power Generation, *ibid.* pp. 37–60.
4. J. K. TIEN, R. M. ARONS and R. W. CLARK, J. *Metals* **28** (12) (1976) 26.
5. R. M. ARONS and J. K. TIEN, "High Temperature Superalloy – Conservation and the Ceramic Alternatives", Proceedings of the Conference in Intermaterials Competition and Resource Availability, 82nd AIChE Meeting, August 1976, AIChE Symposium series, **73**, **170** (1977) pp. 104-105.
6. F. F. LANGE, *Ann. Rev. Mat. Sci.* **4** (1974) 365.
7. I. B. CUTLER and W. J. CROFT, *Powder Met. Int.* **6** (1974) 92, 144.
8. J. W. EDINGTON, D. J. ROWCLIFFE and J. L. HENSHALL, *ibid.* 7 (1975) 82, 136.
9. S. WILD, P. GRIEVESON, K. H. JACK and M. J. LATIMER, The Role of Magnesia in Hot-Pressed Silicon Nitride, "Special Ceramics", Vol. 5, edited by P. Popper (British Ceramic Research Ass., Manchester, 1972) pp. 377.
10. R. F. COE, R. J. LUMBY and M. F. PAWSON, Some Properties and Applications of Hot Pressed Silicon Nitride, *ibid.* pp. 361.
11. I. COLQUHOUN, D. P. THOMPSON, W. I. WILSON,

P. GRIEVESON and K. H. JACK, *Proc. Brit. Ceram. Soc.* **22** (1973) 181.
12. R. J. WESTON and T. G. CARRUTHERS, *ibid.* **22** (1973) 197.
13. G. R. TERWILLIGER and F. F. LANGE, *J. Amer. Ceram. Soc.* **57** (1974) 25.
14. K. H. JACK in "Ceramics for high performance applications", edited by J. J. Burke, A. E. Gorum and R. N. Katz (Brook Hill, Chestnut Hill, Mass., 1974) pp. 265–286.
15. P. DREW and M. H. LEWIS, *J. Amer. Ceram. Soc.* **9** (1974) 261.
16. R. KOSSOWSKY, *ibid.* 8 (1973) 1603.
17. L. K. V. LOU, T. E. MITCHELL and A. H. HEUER, *ibid.* **61** (1978) 392.
18. S. HOFFMANN and L. J. GAUCKLER, *Powder Met. Int.* **6** (1974) 90.
19. K. NUTTALL and D. P. THOMPSON, *J. Mater. Sci.* **9** (1974) 850.
20. D. R. CLARKE and G. THOMAS, *J. Amer. Ceram. Soc.* **60** (1977) 491.
21. A. G. EVANS and R. W. DAVIDGE, *J. Mater. Sci.* **5** (1970) 314.
22. R. KOSSOWSKY, *J. Amer. Ceram. Soc.* **56** (1973) 531.
23. *Idem*, in "Ceramics for high performance applications" edited by J. J. Burke, A. E. Gorum and R. N. Katz (Brook Hill, Chestnut Hill, Mass., 1974) pp. 347–372.
24. R. KOSSOWSKY, D. G. MILLER and E. S. DIAZ, *J. Mater. Sci.* **10** (1975) 983.
25. M. S. SELTZER, *Ceram. Bull.* **56** (1977) 418.
26. F. F. LANGE in "Special Ceramics", Vol. 5, edited by P. Popper (British Ceramic Assn. Manchester, 1972) pp. 361–382.
27. S. PURUSHOTHAMAN and J. K. TIEN, *Acta Met.* **26** (1978) 519.
28. C. A. ANDERSON, D. P. WEI and R. KOSSOWSKY, in "Deformation of Ceramic Materials", edited by R. C. Bradt and R. E. Tessler (Plenum Press, New York, 1975) 383.
29. R. C. NEWNHAM, *Proc. Brit. Ceram. Soc.* **25** (1975) 281.
30. R. G. HOAGLAND, C. W. MARSCHALL and W. H. DUCKWORTH, *J. Amer. Ceram. Soc.* **56** (1976) 189.
31. R. CARLSON, Norton, Co, Worcester, Mass, Private communication.
32. S. UD DIN and P. S. NICHOLSON, *J. Mater. Sci.* **10** (1975) 1375.
33. W. ENGEL, E. GUGEL and F. THÜMMLER, *Sci. Ceramics.* 7 (1973) 415.
34. R. M. ARONS, Appendix I, Eng. Sci. D. Thesis, Columbia University, 1978.
35. E. B. ALLISON, P. BROCK and J. WHITE, *Trans. Brit. Ceram Soc.* **58** (1959) 495.
36. J. E. DORN, The spectrum of Activation Energies for creep, in "Creep and recovery" (American Society for Metals, Cleveland, Ohio, 1957) pp. 255–83.
37. C. O. HULSE and J. A. PASK, *J. Amer. Ceram Soc.* **49** (1966) 312.
38. L. J. TROSTEL, *Ceram. Bull.* **48** (1969) 601.
39. W. ENGEL and F. THÜMMLER, *Ber. Deut. Keram. Ges.* **50** (1973) 204.
40. A. A. SOLOMON in "Special Ceramics", Vol. 5, edited by P. Popper (British Ceramic Assn. Manchester, 1972) pp. 313–324.
41. *Idem, J. Amer. Ceram. Soc.* **56** (1973) 164.
42. D. R. BLAND, "The Theory of Linear Viscoelasticity" (Pergamon Press, New York, 1960).
43. R. MORRELL and K. H. G. ASHBEE, *J. Mater. Sci.* **8** (1973) 1253.
44. D. R. MOSHER, R. RAJ and R. KOSSOWSKY, *ibid.* **11** (1976) 49.

Received 28 March 1979 and accepted 8 January 1980.